A failure mode dependent continuum damage model for laminated composites with optimized model parameters: Application to curved beams

Shubham Rai^{a,*}, Badri Prasad Patel^{a,*}

^aDepartment of Applied Mechanics, Indian Institute of Technology Delhi, Hauz khas, 110016, New Delhi, India

Abstract

In this article, a failure mode dependent and thermodynamically consistent continuum damage model with polynomial-based damage hardening functions is proposed for continuum damage modeling of laminated composite panels. The damage model parameters are characterized based on all uniaxial/shear experimental stress-strain curves. Steepest descent optimization algorithm is used to minimize the difference between model predicted and experimental stress-strain curves to get the optimized model parameters. The fully characterized damage evolution equations are used for damage prediction of a moderately thick laminated composite curved beam modeled using first-order shear deformation theory. Finite element method with load control is used to get the non-linear algebraic equations which are solved using Newton Raphson method. The developed model is compared with the existing failure mode dependent and failure mode independent damage models. The results depict the efficacy of the proposed model to capture non-linearity in the load vs deflection curve due to stiffness degradation and different damage in tension and compression consistent with uniaxial/shear stress-strain response and strength properties of the material, respectively.

Keywords:

Continuum Damage Mechanics, Failure mode dependent, Finite element method, Fiber reinforced composites, Curved beams

1. Introduction

Brittle fiber-reinforced composites undergo stiffness degradation upon application of load due to the evolution of micro-cracks/voids. This stiffness degradation can be modeled using Continuum Damage Mechanics (CDM). The thermodynamically consistent continuum damage models involve damage hardening functions in terms of an equivalent damage parameter to account for the energy dissipation due to damage. Robbins et al. [1] investigated the effect of linear and exponential damage hardening functions on damage evolution and uniaxial/shear stress-strain behavior of fiber reinforced composites using failure mode independent damage model proposed by Barbero and De Vivo [2]. Gupta and Patel [3] used the Barbero and De Vivo [2] damage model with linear damage hardening function for damage prediction of laminated cylindrical/conical panels. To the best of the authors knowledge, the effect of different polynomial-based damage hardening functions (optimized using all uniaxial/shear stress-strain curves) on the damage evolution of laminated composites has not been investigated in the literature to the best of the author's knowledge. Therefore, in the present work, a thermodynamically consistent failure mode-dependent damage model with polynomial-based damage hardening functions and optimized model parameters is proposed for laminated composites, and its application is demonstrated considering laminated composite curved beams.

2. Formulation

2.1. Failure mode dependent continuum damage model development

Fiber-reinforced composites involve different failure mechanisms in different directions (viz. fiber rupture, fiber kinking/micro-buckling, matrix cracking, matrix crushing, delamination, etc.). Failure mode independent damage evolution equations cannot account for these mechanisms accurately. Further, the

^{*}Communicating authors

damage evolution equations can be derived either based on experimental observations (phenomenological damage models) or laws of irreversible thermodynamics. However, the experimental observations to propose damage evolution equations are not always available a priori and involve extensive testing of the material which is cost intensive. Therefore, a three-dimensional thermodynamically consistent failure mode-dependent continuum damage model is developed in this section. The failure modes considered in this paper are fiber rupture, fiber kinking/micro-buckling, matrix cracking, and matrix crushing. The damage is represented by second-order symmetric damage tensor, which is expressed in principal material direction coordinate space in Voigt notation as $\underline{D} = [D_{11} \ D_{22} \ D_{33} \ D_{12} \ D_{13} \ D_{23}]^T$. The subscripts 1, 2, and 3 represent the principal material coordinates of fiber-reinforced composite material in fiber, in-plane, and out-of-plane transverse to fiber direction, respectively. The fourth-order symmetric compliance tensor for an orthotropic composite material depending on the damage variables (based on [4]) is given in contracted notation as:

$$\underline{\underline{H}}(\underline{D}) = \begin{bmatrix}
\frac{1}{E_{1}(1-D_{11})} & -\frac{\nu_{21}}{E_{2}} & -\frac{\nu_{31}}{E_{3}} & 0 & 0 & 0 \\
-\frac{\nu_{21}}{E_{2}} & \frac{1}{E_{2}(1-D_{22})} & -\frac{\nu_{32}}{E_{3}} & 0 & 0 & 0 \\
-\frac{\nu_{31}}{E_{3}} & -\frac{\nu_{32}}{E_{3}} & \frac{1}{E_{3}(1-D_{33})} & 0 & 0 & 0 \\
0 & 0 & 0 & \frac{1}{G_{12}(1-D_{12})} & 0 & 0 & 0 \\
0 & 0 & 0 & 0 & \frac{1}{G_{13}(1-D_{13})} & 0 & 0 \\
0 & 0 & 0 & 0 & 0 & \frac{1}{G_{33}(1-D_{33})}
\end{bmatrix} \tag{1}$$

where E_1 , E_2 and E_3 are Young's moduli of elasticity in fiber, in-plane, and out-of-plane transverse to fiber directions, respectively. G_{12} is in-plane and G_{13} , G_{23} are out-of plane shear moduli of elasticity. The elastic constitutive relation for a lamina with evolving damage is given by $\underline{\sigma} = \underline{\underline{C}}(\underline{D})\underline{\varepsilon}$, where $\underline{\underline{C}} = \underline{\underline{H}}^{-1}(\underline{D})$ is the elastic constitutive tensor depending on damage variable $\underline{\underline{D}}$ and $\underline{\sigma} = [\sigma_{11} \ \sigma_{22} \ \sigma_{33} \ \sigma_{12} \ \sigma_{13} \ \sigma_{23}]^T$, $\underline{\varepsilon} = [\varepsilon_{11} \ \varepsilon_{22} \ \varepsilon_{33} \ 2\varepsilon_{12} \ 2\varepsilon_{13} \ 2\varepsilon_{23}]^T$ are stress and strain tensors expressed in Voigt notation, respectively.

The Helmholtz free energy density of a composite lamina with evolving damage is split into an elastic recoverable strain energy density ϕ_e and a dissipative energy density π depending on an internal state variable β , also known as damage hardening variable. It is expressed as [1, 2]:

$$\psi(\underline{\varepsilon}_e, \underline{D}, \beta) = \frac{1}{\rho} (\phi_e(\underline{\varepsilon}_e, \underline{D}) + \pi(\beta))$$
 (2)

For the same state of damage (\underline{D}) and elastic strain $(\underline{\varepsilon}_e)$, there can be different amounts of energy dissipation depending on the micro-structure or grain structure of the material (Fig. 1). Therefore, an independent variable β is required to account for the amount of energy dissipation.

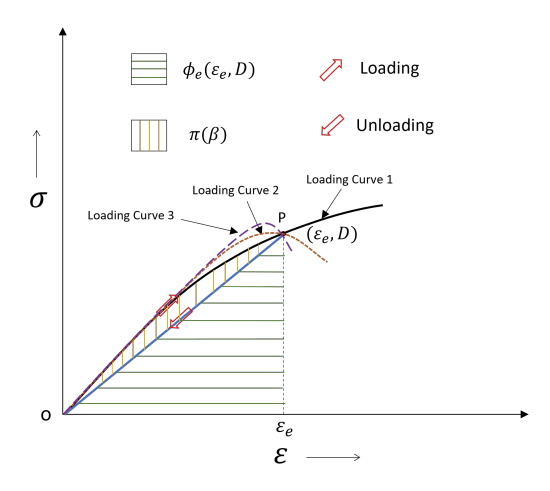


Figure 1: Representation of recoverable (ϕ_e) and dissipative (π) energy densities

2.1.1. Damage evolution equations

Damage evolution equations are derived based on laws of irreversible thermodynamics without resorting to experimental observations a priori. The second law of thermodynamics invoking isothermal conditions, elastic deformation with evolving damage and zero heat flux exchange, is given in terms of Clausius-Duhem inequality as [5]:

$$\left(\underline{\sigma} - \frac{\partial(\rho\psi)}{\partial\underline{\varepsilon}_e}\right)\underline{\dot{\varepsilon}}_e - \frac{\partial(\rho\psi)}{\partial\underline{D}}\underline{\dot{D}} - \frac{\partial(\rho\psi)}{\partial\beta}\dot{\beta} \ge 0 \tag{3}$$

The thermodynamic damage driving force (\underline{Y}) conjugate to damage variable \underline{D} and damage hardening function (γ) conjugate to damage hardening variable β are defined as:

$$\underline{Y} = -\frac{\partial(\rho\psi)}{\partial\underline{D}} = -\frac{\partial\phi_e}{\partial\underline{D}} = \frac{\partial\chi}{\partial\underline{D}} = \frac{1}{2}\underline{\sigma} : \frac{\partial\underline{\underline{H}}(\underline{D})}{\partial\underline{D}} : \underline{\sigma}$$

$$\tag{4}$$

$$\gamma(\beta) = \frac{\partial(\rho\psi)}{\partial\beta} = \frac{\partial(\pi)}{\partial\beta} \tag{5}$$

where $\chi(\underline{\sigma}, \underline{D})$ is complementary energy density.

Substituting Eqs. 4, 5 in Eq. 3 and considering the arbitrary nature of $\dot{\varepsilon}_e$ gives :

$$\underline{\sigma} = \frac{\partial(\rho\psi)}{\partial\varepsilon_{\alpha}} \tag{6}$$

$$\Phi(\underline{Y}, \gamma) = Y_i \dot{D}_i - \gamma \dot{\beta} \ge 0 \tag{7}$$

where $\Phi(\underline{Y}, \gamma)$ is known as damage dissipation power density. The dissipation power density is considered to be failure mode dependent and the principle of maximum dissipation (subject to consistency condition $f_m(\underline{Y}) = 0$, where m represents damage mode) is used to arrive at failure mode dependent damage evolution equations in m^{th} mode. f_m denotes the loading criteria function in m^{th} mode in thermodynamic damage driving force (\underline{Y}) space. Lagrange multiplier approach is used to maximize $\Phi_m(\underline{Y}, \gamma_m)$ subject to $f_m(\underline{Y}) = 0$, where the subscript m=1: ft, 2: fc, 3: mt and 4: mc for fiber tension, fiber compression, matrix tension and matrix compression mode, respectively. The unconstrained objective function is expressed as:

$$\Phi_m^*(\underline{Y}, \gamma_m) = \underline{Y}.\underline{\dot{D}}_m - \gamma_m \dot{\beta}_m - \lambda f_m \tag{8}$$

where λ is Lagrange multiplier and repeated index m does not imply summation. The first-order necessary condition for maxima of ϕ_m^* give :

$$\underline{\dot{D}}_m = \dot{\beta}_m \frac{\partial f_m}{\partial Y} \tag{9}$$

The total increment in damage is the summation of incremental damage variables from each mode as:

$$\underline{\dot{D}} = \sum_{m=1}^{4} \dot{\beta}_m \frac{\partial f_m}{\partial \underline{Y}} \tag{10}$$

2.2. Loading criteria functions

The loading criteria functions (based on [4, 6, 7]), with different damage hardening functions and damage hardening variable in each mode, are expressed in four modes of damage in stress space as:

Fiber Tension $(\sigma_{11} > 0)$:

$$f_1 = \left(\frac{\sigma_{11}}{(1 - D_{11})X_t}\right)^2 + \left(\frac{\sigma_{12}}{(1 - D_{12})S_a}\right)^2 + \left(\frac{\sigma_{13}}{(1 - D_{13})S_a}\right)^2 - \gamma_1(\beta_1) = \underline{\sigma}^T \underline{\underline{F_1}}\underline{\sigma} - \gamma_1(\beta_1)$$
(11)

Fiber Compression ($\sigma_{11} < 0$):

$$f_2 = \left(\frac{\sigma_{11}}{(1 - D_{11})X_c}\right)^2 - \gamma_2(\beta_2) = \underline{\underline{\sigma}}^T \underline{\underline{F_2}}\underline{\underline{\sigma}} - \gamma_2(\beta_2) \tag{12}$$

Matrix Tension $(\sigma_{22} + \sigma_{33}) > 0$:

$$f_{3} = \left(\frac{\sigma_{22}}{(1 - D_{22})Y_{t}}\right)^{2} + \left(\frac{\sigma_{33}}{(1 - D_{33})Z_{t}}\right)^{2} + \left(\frac{\sigma_{12}}{(1 - D_{12})S_{a}}\right)^{2} + \left(\frac{\sigma_{13}}{(1 - D_{13})S_{a}}\right)^{2} + \left(\frac{\sigma_{23}}{(1 - D_{23})S_{t}}\right)^{2} - \gamma_{3}(\beta_{3}) = \underline{\sigma}^{T} \underline{F_{3}}\underline{\sigma} - \gamma_{3}(\beta_{3})$$

$$(13)$$

Matrix Compression $(\sigma_{22} + \sigma_{33}) < 0$:

$$f_{4} = \left(\frac{\sigma_{22}}{(1 - D_{22})Y_{c}}\right)^{2} + \left(\frac{\sigma_{33}}{(1 - D_{33})Z_{c}}\right)^{2} + \left(\frac{\sigma_{12}}{(1 - D_{12})S_{a}}\right)^{2} + \left(\frac{\sigma_{13}}{(1 - D_{13})S_{a}}\right)^{2} + \left(\frac{\sigma_{23}}{(1 - D_{23})S_{t}}\right)^{2} - \gamma_{4}(\beta_{4}) = \underline{\sigma}^{T} \underline{F_{4}}\underline{\sigma} - \gamma_{4}(\beta_{4})$$

$$(14)$$

where X_t, X_c are strength in fiber tension and compression, respectively, Y_t, Y_c are strength in in-plane transverse to fiber tension and compression, respectively, Z_t, Z_c are strength in out-of-plane transverse to fiber tension and compression, respectively. $S_a = S_{12} = S_{13}$ is the axial shear strength of the lamina and $S_t = S_{23}$ is the transverse shear strength of the lamina. Tensors $\underline{F_1}, \underline{F_2}, \underline{F_3}$ and $\underline{F_4}$ are defined in appendix. The thermodynamic damage driving force in eq. 4 in stress tensor $\underline{(\sigma)}$ and damage variable tensor $\underline{(D)}$ space is written as:

$$\underline{Y}(\underline{\sigma}, \underline{D}) = [Y_{11}, Y_{22}, Y_{33}, Y_{12}, Y_{13}, Y_{23}]^{T}
= \left[\frac{\sigma_{11}^{2}}{2(1 - D_{11})^{2} E_{1}}, \frac{\sigma_{22}^{2}}{2(1 - D_{22})^{2} E_{2}}, \frac{\sigma_{33}^{2}}{2(1 - D_{33})^{2} E_{3}}, \frac{\sigma_{12}^{2}}{2(1 - D_{12})^{2} G_{12}}, \frac{\sigma_{13}^{2}}{2(1 - D_{13})^{2} G_{13}}, \frac{\sigma_{23}^{2}}{2(1 - D_{23})^{2} G_{23}}\right]$$
(15)

The loading criteria functions $f_m(\underline{\sigma})$ are converted from stress space to thermodynamic damage driving force space $f_m(\underline{Y})$ using Eq. 15 as:

$$f_1 = \frac{2Y_{11}E_1}{X_t^2} + \frac{2Y_{12}G_{12}}{S_a^2} + \frac{2Y_{13}G_{13}}{S_a^2} - \gamma_1(\beta_1)$$
 (16)

$$f_2 = \frac{2Y_{11}E_1}{X_2^2} - \gamma_2(\beta_2) \tag{17}$$

$$f_3 = \frac{2Y_{22}E_2}{Y_t^2} + \frac{2Y_{33}E_3}{Z_t^2} + \frac{2Y_{12}G_{12}}{S_a^2} + \frac{2Y_{13}G_{13}}{S_a^2} + \frac{2Y_{23}G_{23}}{S_t^2} - \gamma_3(\beta_3)$$
(18)

$$f_4 = \frac{2Y_{22}E_2}{Y_c^2} + \frac{2Y_{33}E_3}{Z_c^2} + \frac{2Y_{12}G_{12}}{S_a^2} + \frac{2Y_{13}G_{13}}{S_a^2} + \frac{2Y_{23}G_{23}}{S_t^2} - \gamma_4(\beta_4)$$
(19)

Finally, the thermodynamic damage driving force in stress space $\underline{Y}(\underline{\sigma},\underline{D})$ is expressed in strain space, i.e. $\underline{Y}(\underline{\varepsilon},\underline{D})$, using the constitutive relation $\underline{\sigma} = (\underline{C}(\underline{D}))\underline{\varepsilon}$.

2.2.1. Damage hardening functions

Due to different mechanisms of damage evolution in different directions in fiber-reinforced composite materials, there is a need to propose different damage hardening variables (β_m) in each mode m. Polynomial-based damage hardening functions are selected based on the minimum difference between the model predicted and experimental uniaxial/shear stress-strain curves in the numerical characterization of damage model parameters. Three types of damage hardening functions are taken, i.e., linear, quadratic, and cubic polynomials, with damage hardening function parameters dependent on damage mode m. The damage hardening functions are expressed as:

$$\gamma_m(\beta_m) = C_{1m}\beta_m + C_{2m}\beta_m^2 + C_{3m}\beta_m^3 \tag{20}$$

For linear damage hardening: $C_{1m} > 0$, $C_{2m} = 0$ and $C_{3m} = 0$

For quadratic damage hardening : $C_{1m} > 0$, $C_{2m} > 0$ and $C_{3m} = 0$

For cubic damage hardening: $C_{1m} > 0$, $C_{2m} > 0$ and $C_{3m} > 0$

The damage evolution equations are solved iteratively using the value of strain ($\underline{\varepsilon}$) at the current iteration and the damage variable value obtained from the previous iteration to get the damage variable at the current iteration by satisfying loading criteria ($f_m(\underline{Y}) = 0$) in each mode.

2.3. Damage model parameter characterization of the developed failure mode dependent damage model

The linear, quadratic, and cubic polynomial-based damage hardening functions are considered for optimization of model parameters of the proposed three-dimensional thermodynamically consistent failure mode dependent continuum damage model (with damage evolution equations involving six damage variables $D_{11}, D_{22}, D_{33}, D_{12}, D_{13}$ and D_{23} , derived based on second law of thermodynamics by simultaneously satisfying the loading criteria by using functions derived based on Hashin (1980) [6] failure criteria) to minimize the difference between model predicted and experimental uniaxial/shear stress-strain curves. Steepest descent algorithm (for optimization) coupled with Newton-Raphson iterative procedure (for solving damage evolution equations by satisfying loading criteria) is used to arrive at an optimized set of damage model parameters $\mathcal{P} = [C_{1m} \ C_{2m} \ C_{3m}]$. The loss/objective function based on the squared difference between the model predicted and experimental uniaxial/shear stress-strain curve is given as:

$$\mathcal{L}_{m_a}(\underline{\mathcal{P}}) = \sum_{j=1}^{n_{m_a}} \sum_{i=1}^{n} \left(\frac{\sigma_{(j)exp}^i - \sigma_{(j)model}^i(\underline{\mathcal{P}})}{S_j} \right)^2$$
 (21)

where i and j represent summation over experimental data points and number of active stress-strain curves, respectively. S_j represents strength value in j^{th} uniaxial/shear stress-strain curve. The summation of the active mode dependent loss function over all the possible combinations of active modes (m_a) gives the total loss function $\mathcal{L}(\mathcal{P})$.

AS4/3501-6 fiber reinforced brittle composite with material properties taken from [8] and [9] (Table 1) is considered for the analysis. The model predicted, and experimental in-plane normal and out-of-plane shear stress vs strain curves with linear, quadratic, and cubic damage hardening for the damage modes active in fiber tension - matrix tension (ft - mt) and fiber compression - matrix compression (fc - mc) are shown in Fig. 2 and Fig. 3, respectively. These curves depict that the damage hardening function with a polynomial up to cubic terms gives the most accurate results. Damage variable vs. strain curves corresponding to cubic damage hardening (Fig. 2) depicts more damage in the out-of-plane shear direction.

The optimized damage model parameters and active mode dependent loss function values for cubic damage hardening are given as:

$$\begin{array}{l} C_{1ft} = 0.1027 \times 10^{-4}, \ C_{2ft} = 0.3354 \times 10^{-14}, \ C_{3ft} = 0.2105 \times 10^{-15} \\ C_{1mt} = 0.5966 \times 10^{-9}, \ C_{2mt} = 0.1203 \times 10^{-14}, \ C_{3mt} = 0.2263 \times 10^{-12} \\ \pounds_{ft-mt}(\underline{\mathcal{P}}) = 0.03442 \end{array}$$

$$C_{1fc} = 0.1276 \times 10^{-5}, C_{2fc} = 0.5388 \times 10^{-12}, C_{3fc} = 0.4125 \times 10^{-18}$$

 $C_{1mc} = 0.1274 \times 10^{-4}, C_{2mc} = 0.2904 \times 10^{-14}, C_{3mc} = 0.2735 \times 10^{-16}$
 $\pounds_{fc-mc}(\mathcal{P}) = 0.236149$

Elastic Properties	Values	Strength Properties	Values
$\overline{E_1}$	140.4 GPa	X_t	1980 MPa
$E_2 = E_3$	11 GPa	X_c	$1200~\mathrm{MPa}$
$G_{12} = G_{13}$	6.60 GPa	Y_t	53 MPa
G_{23}	3.62 GPa	Y_c	200 MPa
$\nu_{12} = \nu_{13}$	0.28	$S_a = S_{12} = S_{13}$	79 MPa
$ u_{23}$	0.52	$S_t = S_{23}$	55 MPa

Table 1: Material Properties for AS4/3501-6 fiber-reinforced composite [8, 9]

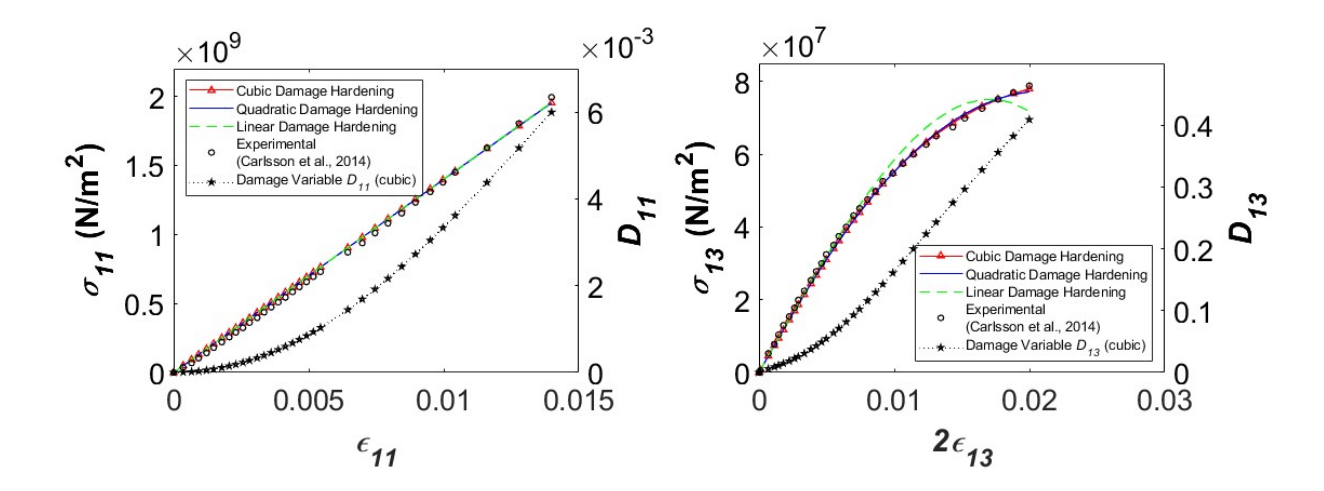


Figure 2: Experimental versus optimized model predicted stress-strain curves and damage variable vs strain curves corresponding to linear, quadratic and cubic damage hardening for the ft-mt active set of damage modes.

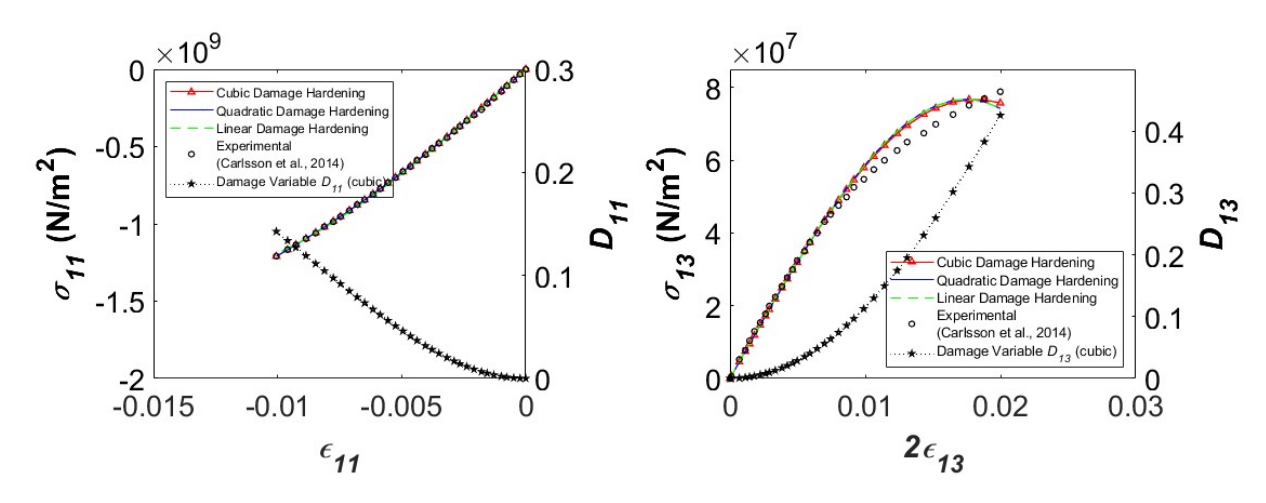


Figure 3: Experimental versus optimized model predicted stress-strain curves and damage variable vs strain curves corresponding to linear, quadratic and cubic damage hardening for the fc - mc active set of damage modes.

3. Finite Element Formulation

First-order shear deformation theory is used for modeling a moderately thick laminated composite curved panel subjected to transverse loading. The geometry and coordinate system of the panel are shown in Fig. 4 where R is the radius of curvature of the panel, L is the length of the panel along θ coordinate and φ is the sector angle of the panel such that $L = R \varphi$.

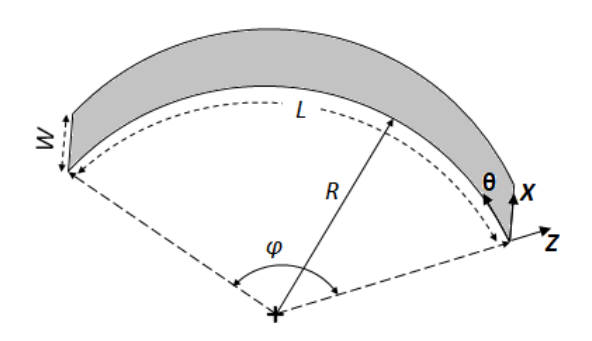


Figure 4: Geometry and coordinate system of a curved panel

The displacements u, v and w along the x, θ and z directions, respectively are given as:

$$u(x, \theta, z) = u_o(x, \theta) + z\psi_x(x, \theta)$$

$$v(x, \theta, z) = v_o(x, \theta) + z\psi_\theta(x, \theta)$$

$$w(x, \theta, z) = w_o(x, \theta)$$
(22)

where u_o , v_o and w_o are mid-plane displacements. ψ_x and ψ_θ are the rotations of shell normal about θ and negative x axes, respectively.

The strain displacement relationship based on the assumptions of (i) small strains and rotations, and (ii) thin shells $(1 + z/R \approx 1)$ are given as:

$$\left\{\varepsilon\right\} = \begin{cases} \varepsilon_{xx} \\ \varepsilon_{\theta\theta} \\ \gamma_{x\theta} \\ \gamma_{xz} \\ \gamma_{\thetaz} \end{cases} = \begin{cases} \frac{\partial u_o}{\partial x} \\ \frac{1}{R} \frac{\partial v_o}{\partial \theta} + \frac{w_o}{R} \\ \frac{1}{R} \frac{\partial u_o}{\partial \theta} + \frac{\partial v_o}{\partial x} \\ 0 \\ 0 \end{cases} + \begin{cases} z \frac{\partial \psi_a}{\partial x} \\ \frac{z}{R} \frac{\partial \psi_\theta}{\partial \theta} \\ \frac{z}{R} \frac{\partial \psi_\theta}{\partial \theta} + z \frac{\partial \psi_\theta}{\partial x} \\ \psi_x + \frac{\partial w_o}{\partial x} \\ \psi_\theta + \frac{1}{R} \frac{\partial w_o}{\partial \theta} - \frac{v_o}{R} \end{cases}$$
(23)

The whole geometry is discretized into C^0 continuous finite elements. All the numerical integrations are performed using Gauss Quadrature numerical integration scheme with 3×3 Gauss points for integration with respect to x and θ , and 5 Gauss points in each layer for integration with respect to z. The total load is applied in a number of steps to ensure convergence of nodal degrees of freedom within each load step. Every load step involves global iterations in which the damage evolution equations are solved iteratively at each Gauss point using the strain values at the current global iteration by satisfying the loading criteria $f_m = 0$.

4. Results and discussion

The above formulation is used for damage prediction in a laminated composite curved beam (L/W=1000) with a lamination scheme as 90/90/90/90 with respect to x coordinate, i.e., the direction of fibers in all four layers are along θ direction. The dimensions of the beam are : $\varphi=0.4$ rad, R=4m i.e. L=1.6m, L/h=10 where h is the thickness of the beam. The material properties are taken from Table. 1. Both sides of the beam are clamped to restrict all the displacement and rotation degrees of freedom, and the beam is subjected to uniformly distributed transverse load in the positive z direction (radially outward).

The present failure mode dependent damage model is compared with the failure mode independent damage model of Barbero and De Vivo [2] with constitutive relations taken from [1] and an existing uncoupled form of phenomenological failure mode dependent damage model [10] with compliance matrix given by Eq. 1 . A mesh size of 10×1 is taken for the present and Barbero and De Vivo damage models. A mesh size of 1000×1 is taken for the existing failure mode-dependent damage model based prediction. The damage model parameters for Barbero and De Vivo damage model are taken from Rai and Patel [11] and are given in Table 2. Babero's associative damage model ($H_1 = H_2 = H_3 = 0$) with linear damage hardening is considered for damage prediction of the curved beam.

The damage evolution equations of the existing failure mode dependent damage model (based on Pan et al. [10]) are given as:

$$d_i^j = 1 - \frac{1}{f_i^j} \exp \frac{(1 - f_i^j)\varepsilon_{fi}^j S_i^j l_c}{G_{ci}^j}$$

$$\tag{24}$$

where i=f (fiber), m (matrix) and j=t (tension), c (compression), S represents the strength, f_i^j is the failure criteria function, ε_f represents the failure strain, l_c is the characteristic length of the element taken as square root of integration point area [12, 13] ($l_c=0.0005333$ for the considered mesh size) and G_c is the fracture energy. Also, $d_f^j=D_{11}, d_m^j=D_{22}, D_{33}, D_{12}=1-(1-D_{11})(1-D_{22}), D_{13}=1-(1-D_{11})(1-D_{33})$ and $D_{23}=1-(1-D_{22})(1-D_{33})$. The strength properties required for this model are taken from Table 1, fracture toughness values are taken from [14] and are given as: $G_{cf}^t=91,600 \text{ J/m}^2, G_{cf}^c=79,900 \text{ J/m}^2, G_{cm}^t=220 \text{ J/m}^2$ and $G_{cm}^c=760 \text{ J/m}^2$, failure strains are taken from [8] and are given as: $\varepsilon_{ff}^t=0.014, \varepsilon_{ff}^t=0.01, \varepsilon_{fm}^t=0.0055$ and $\varepsilon_{fm}^c=0.02$.

$\pounds, \underline{\mathcal{P}}$	Linear Hardening	$\underline{\mathcal{P}}$	Values
£	0.021388	J_{11}	1.7588×10^{-15}
C_1	5.8573×10^{-7}	$J_{22} = J_{33}$	1.8263×10^{-13}
C_2	0	H_1	1.0302×10^{-8}
C_3	0	$H_2 = H_3$	-7.8913×10^{-9}

Table 2: Damage model parameters and loss function values for failure mode independent damage model [2] for AS4/3501-6 composite material [11].

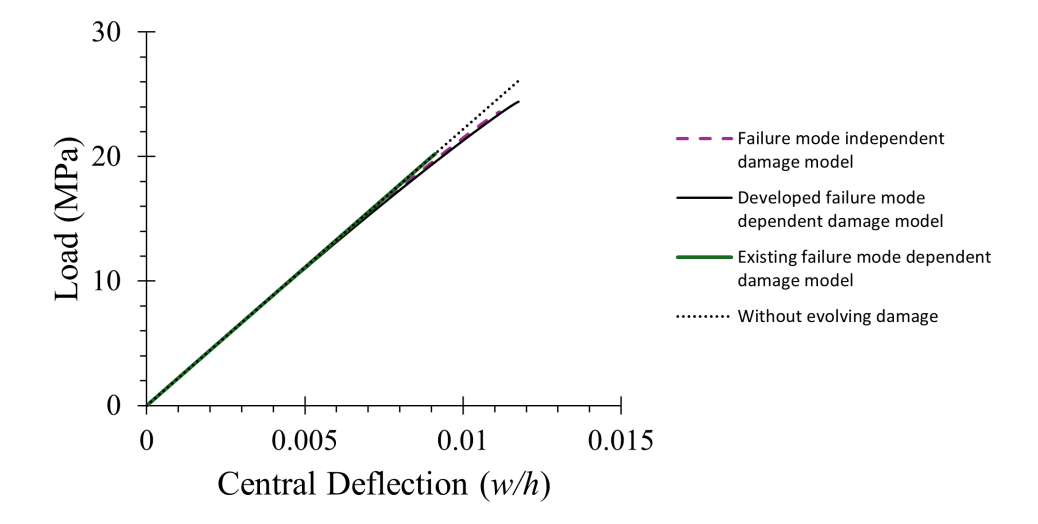


Figure 5: Load vs central deflection of the curved laminated composite beam (90/90/90/90) for the Present damage model, and Barbero and De Vivo [2] associative damage model and an exisiting failure mode dependent damage model [10].

The load vs central deflection for the laminated composite curved beam is shown in Fig. 5 for the proposed damage model with cubic damage hardening, the Barbero and De Vivo [2] associative damage model with linear damage hardening and the existing failure mode dependent phenomenological damage model [10]. The figure depicts the stiffness degradation of laminated composite curved beam due to damage evolution with failure loads (failure load is the load when either the damage variable reaches one or there is convergence failure of the employed load control algorithm) as 24.39 MPa, 23.56 MPa and 20.24 MPa for the proposed damage model, Barbero and De Vivo [2] associative damage model and existing failure mode dependent damage model, respectively.

The existing failure mode dependent damage model [10] involves damage evolution when failure criteria function f_i^j at any Gauss point is greater than 1 (which is satisfied after 19.3 MPa for the present geometry, loading, and boundary conditions). Also, the damage variable vs strain curve is concave downward for the existing failure mode-dependent damage model, leading to a rapid damage evolution at the beginning. Therefore, the load vs central deflection curve is almost linear for this model.

Significant non-linearity in load vs central deflection curves is predicted by the developed failure mode dependent damage model and Barbero and De Vivo [2] failure mode independent damage model. Although the failure loads for both the damage models are fairly close, there is a significant difference between the distribution of damage variables D_1, D_3 (Barbero and De Vivo model [2]) and D_{11}, D_{33} (present developed model).

The damage evolution equations of Barbero and De Vivo damage model [2] and the present damage model involve coupling vectors which account for coupling among different damage variables at a material point. The coupling vector of Barbero and De Vivo associative damage model (Eqns. 9 and 14 of [1]) involve participation of in-plane normal strain ε_{11} and out of plane shear strain $2\varepsilon_{13}$ for the evolution of damage variable D_1 and only out of plane shear strain for the evolution of damage variable D_3 . This leads to more evolution of D_1 compared to D_3 as shown in Fig. 6a and 6c. However, the coupling vector of the proposed failure mode dependent associative damage model involves different constant terms (independent of stress and strain) with more evolution of D_{13} compared to D_{11} at a particular material point which is evident in Fig. 6b and 6d. However, the overall degradation of both the damage models is nearly same with Barbero and De Vivo model predicting slightly smaller stiffness degradation than the present model

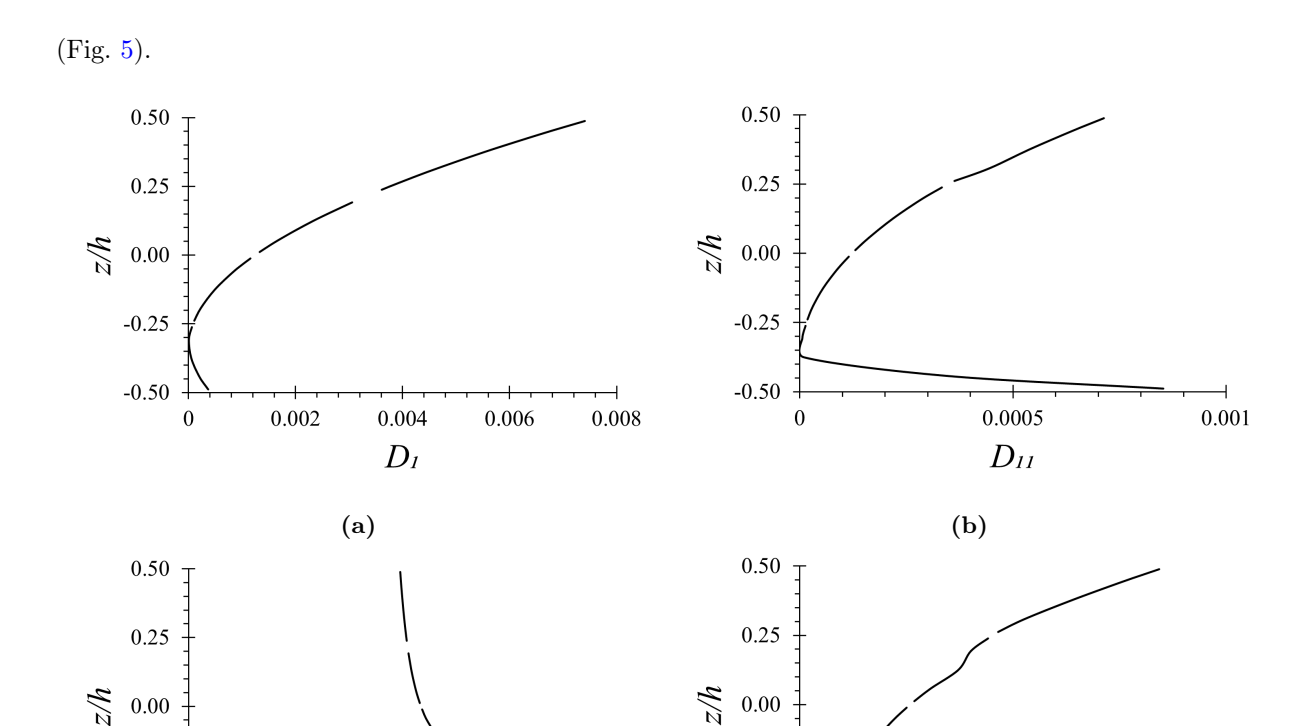


Figure 6: Through the thickness variation of damage variables D_1 , D_3 and D_{11} , D_{13} at the center of the beam for (a),(c) Barbero and De Vivo [2] associative damage model (Applied Load = 23.56 MPa) and (b),(d) Proposed damage model (Applied load = 24.39 MPa)

0.00018

-0.25

-0.50 + 0

0.00006

(c)

0.00012

 D_3

-0.25

-0.50

0.005

0.01

(d)

0.015

 D_{13}

0.02

0.025

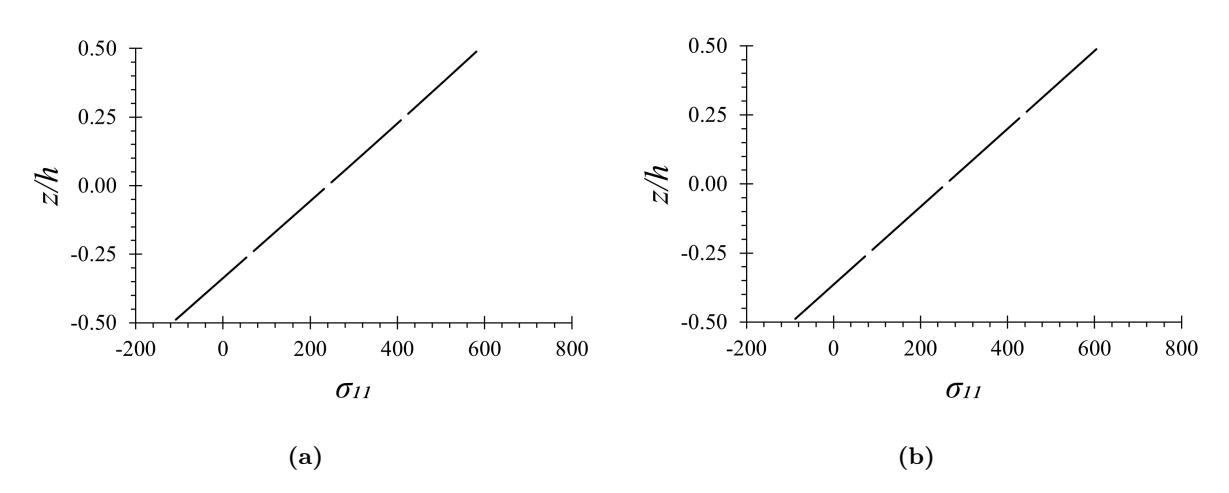


Figure 7: Through the thickness variation of in-plane stress σ_{11} vs z/h at the center of the beam for (a) Barbero and De Vivo [2] associative damage model (Applied load = 23.56 MPa) and (b) Proposed damage model (Applied Load = 24.39 MPa).

Through the thickness variation of the damage variable responsible for stiffness degradation in fiber direction (Fig. 6), at the center of the curved beam, depicts that the present damage model (Fig. 6b) predicts the evolution of damage consistent with the strength properties of the material (Table 1) with more damage in fiber direction compression compared to tension. However, Barbero and De Vivo's damage model is not able to capture the evolution of damage consistent with the strength properties of the material because the damage evolution equations are failure mode independent and driven by the stress magnitude (σ_{11} more in fiber tension compared to fiber compression as shown in Fig. 7)

whereas the proposed damage model takes into account the mode of failure in fiber reinforced composite materials.

5. Conclusions

A three-dimensional thermodynamically consistent and failure mode-dependent damage model with different damage hardening variables in each of the damage modes and polynomial-based damage hardening functions is proposed in this article for fiber-reinforced composite materials. The damage model parameters are characterized using the steepest descent optimization algorithm to minimize the difference between the model predicted and experimental uniaxial/shear stress-strain curves. The optimized damage model is used for stiffness degradation prediction of a laminated composite curved beam subjected to a uniformly distributed transverse load. The proposed damage model is also compared with a failure mode independent Barbero and De Vivo [2] associative damage model and an existing failure mode dependent damage model [10]. Through the thickness variation of the damage variable at the center of the beam depicts that unlike Barbero and De Vivo damage model, the present damage model is able to capture evolution of damage consistent with the strength properties of the material depicting its failure mode dependent nature. Also, the developed model predicts significant non-linearity in the load vs deflection curve, thereby accounting for stiffness degradation due to micro-crack evolution. The developed damage model can be coupled with cohesive zone modeling to account for delamination damage at the interface of the two laminae and will be taken up as a future work.

References

- [1] D. Robbins Jr, J. Reddy, F. Rostam-Abadi, An efficient continuum damage model and its application to shear deformable laminated plates, Mechanics of Advanced Materials and Structures 12 (2005) 391–412.
- [2] E. Barbero, L. De Vivo, A constitutive model for elastic damage in fiber-reinforced pmc laminae, International Journal of Damage Mechanics 10 (2001) 73–93.
- [3] A. Gupta, B. Patel, Y. Nath, Continuum damage mechanics approach to composite laminated shallow cylindrical/conical panels under static loading, Composite Structures 94 (2012) 1703–1713.
- [4] A. Matzenmiller, J. Lubliner, R. L. Taylor, A constitutive model for anisotropic damage in fiber-composites, Mechanics of materials 20 (1995) 125–152.
- [5] L. Hao, P. Ke, W. June, An anisotropic damage criterion for deformation instability and its application to forming limit analysis of metal plates, Engineering Fracture Mechanics 21 (1985) 1031–1054.
- [6] Z. Hashin, Failure criteria for unidirectional fiber composites, Journal of Applied Mechanics 47 (1980) 329–334.
- [7] J. C. Sosa, S. Phaneendra, J. J. Muñoz, Modelling of mixed damage on fibre reinforced composite laminates subjected to low velocity impact, International Journal of Damage Mechanics 22 (2013) 356–374.
- [8] A. Kaddour, M. J. Hinton, P. A. Smith, S. Li, Mechanical properties and details of composite laminates for the test cases used in the third world-wide failure exercise, Journal of Composite Materials 47 (2013) 2427–2442.
- [9] L. A. Carlsson, D. F. Adams, R. B. Pipes, Experimental characterization of advanced composite materials, CRC press, 2014.
- [10] Z. Pan, L. Zhang, K. Liew, The use of curvilinear fibers for enhancement of progressive failure performance of perforated composite panels, Composite Structures 288 (2022) 115424.
- [11] S. Rai, B. P. Patel, A failure mode dependent continuum damage model for thick laminated composite plates, Mechanics of Materials 186 (2023) 104790.
- [12] P. Maimi, P. P. Camanho, J. Mayugo, C. Davila, A continuum damage model for composite laminates: Part ii-computational implementation and validation, Mechanics of materials 39 (2007) 909–919.
- [13] I. Lapczyk, J. A. Hurtado, Progressive damage modeling in fiber-reinforced materials, Composites Part A: Applied Science and Manufacturing 38 (2007) 2333–2341.

[14] E.-H. Kim, M.-S. Rim, I. Lee, T.-K. Hwang, Composite damage model based on continuum damage mechanics and low velocity impact analysis of composite plates, Composite Structures 95 (2013) 123–134.